

Four-Neutrino Scenarios*

C. Giunti[†]

INFN, Sez. di Torino, and Dip. di Fisica Teorica, Univ. di Torino, I-10125 Torino, Italy

The main features of four-neutrino 3+1 and 2+2 mixing schemes are reviewed, after a discussion on the necessity of at least four massive neutrinos if the solar, atmospheric and LSND anomalies are due to neutrino oscillations.

1. Introduction

Solar and atmospheric neutrino experiments have observed for a long time anomalies that are commonly interpreted as evidences in favor of neutrino oscillations with mass squared differences

$$10^{-11} \text{ eV}^2 \lesssim \Delta m_{\text{SUN}}^2 \lesssim 10^{-4} \text{ eV}^2, \quad (1)$$

$$10^{-3} \text{ eV}^2 \lesssim \Delta m_{\text{ATM}}^2 \lesssim 10^{-2} \text{ eV}^2, \quad (2)$$

respectively (see Refs.[1,2]). More recently, the accelerator LSND experiment has reported the observation of $\bar{\nu}_\mu \rightarrow \bar{\nu}_e$ and $\nu_\mu \rightarrow \nu_e$ appearance [3] with a mass-squared difference

$$10^{-1} \text{ eV}^2 \lesssim \Delta m_{\text{LSND}}^2 \lesssim 10 \text{ eV}^2. \quad (3)$$

The LSND evidence in favor of neutrino oscillations has not been confirmed by other experiments, but it has not been excluded either. Awaiting an independent check of the LSND result, that will probably come soon from the Mini-BooNE experiment [3], it is interesting to consider the possibility that the results of solar, atmospheric and LSND experiments are due to neutrino oscillations. In this case, the existence of the three mass-squared differences (1)–(3) with different scales implies that there are at least four massive neutrinos (three massive neutrinos are not enough because the three Δm^2 's have different scales and do not add up to zero).

Since the mass-squared differences (1)–(3) have been obtained by analyzing separately the data

of each type of experiment (solar, atmospheric and LSND) in terms of two-neutrino mixing, it is legitimate to ask if three different mass squared are really necessary to fit the data. The answer is “yes”, as explained in Section 2.

Although the precise measurement of the invisible width of the Z boson has determined that there are only three active flavor neutrinos, ν_e, ν_μ, ν_τ , the possible existence of at least four massive neutrinos is not a problem, because in general flavor neutrinos are not mass eigenstates, *i.e.* there is *neutrino mixing* (see, *e.g.*, Ref.[4]).

In general, the left-handed component $\nu_{\alpha L}$ of a flavor neutrino field is a linear combination of the left-handed components ν_{kL} of neutrino fields with masses m_k : $\nu_{\alpha L} = \sum_k U_{\alpha k} \nu_{kL}$, where U is the unitary neutrino mixing matrix. The number of massive neutrinos is only constrained to be ≥ 3 . Following the old principle known as *Occam razor*, we consider the simplest case of four massive neutrinos that allows to explain all data with neutrino oscillations [5]. In this case, in the flavor basis the usual three active neutrinos ν_e, ν_μ, ν_τ , are associated with a sterile neutrino, ν_s , that is a singlet of the electroweak group.

Taking into account the measured hierarchy

$$\Delta m_{\text{SUN}}^2 \ll \Delta m_{\text{ATM}}^2 \ll \Delta m_{\text{LSND}}^2, \quad (4)$$

there are only six types of possible four-neutrino schemes, which are shown in Fig.1. These six schemes are divided in two classes: 3+1 and 2+2. In both classes there are two groups of neutrino masses separated by the LSND gap, of the order of 1 eV, such that the largest mass-squared difference generates the oscillations observed in the LSND experiment: $\Delta m_{\text{LSND}}^2 = |\Delta m_{41}^2|$ (where $\Delta m_{kj}^2 \equiv m_k^2 - m_j^2$). In 3+1 schemes there is a

*Talk presented at NOW 2000, Conca Specchiulla (Otranto, Italy), 9-16 Sep. 2000; DFTT 47/00, hep-ph/0012236.

[†]I would like to thank G. Mills and B. Louis for useful information on the LSND experiment.

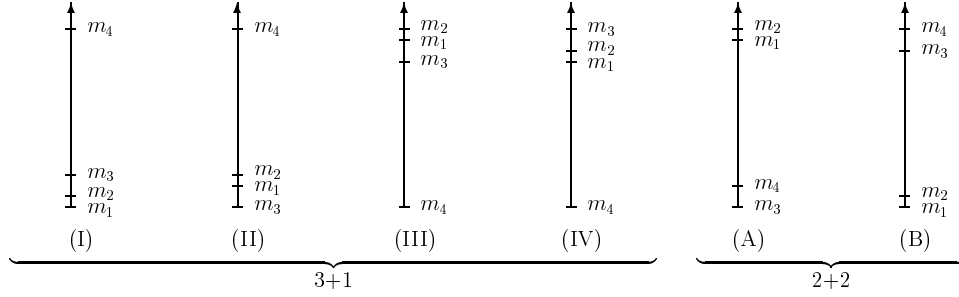


Figure 1. Qualitative illustration of the possible four-neutrino schemes.

group of three neutrino masses separated from an isolated mass by the LSND gap. In 2+2 schemes there are two pairs of close masses separated by the LSND gap. The numbering of the mass eigenvalues in Fig. 1 is conveniently chosen in order to have always solar neutrino oscillations generated by $\Delta m_{21}^2 = \Delta m_{\text{SUN}}^2$. In 3+1 schemes atmospheric neutrino oscillations are generated by $|\Delta m_{31}^2| \simeq |\Delta m_{32}^2| = \Delta m_{\text{ATM}}^2$, whereas in 2+2 schemes they are generated by $|\Delta m_{43}^2| = \Delta m_{\text{ATM}}^2$.

In 1999 the 3+1 schemes were rather strongly disfavored by the experimental data, with respect to the 2+2 schemes [6]. In June 2000 the LSND collaboration presented the results of a new improved analysis of their data, leading to an allowed region in the $\sin^2 2\vartheta - \Delta m^2$ plane (ϑ is the two-generation mixing angle) that is larger and shifted towards lower values of $\sin^2 2\vartheta$, with respect to the 1999 allowed region. This implies that the 3+1 schemes are now marginally compatible with the data. Therefore, in Section 3 I discuss the 3+1 schemes, that have been recently revived [7–9]. In Section 4 I discuss the 2+2 schemes, that are still favored by the data.

2. Three Δm^2 's are necessary

Let us consider the general expression of the probability of $\nu_\alpha \rightarrow \nu_\beta$ transitions in vacuum valid for any number of massive neutrinos:

$$P_{\nu_\alpha \rightarrow \nu_\beta} = \left| \sum_k U_{\alpha k}^* U_{\beta k} \exp \left(-i \frac{\Delta m_{kj}^2 L}{2E} \right) \right|^2, \quad (5)$$

where L is the source-detector distance, E is the neutrino energy, and j is anyone of the mass eigenstate indices (a phase common to all terms in the sum in Eq.(5) is irrelevant).

If all the phases $\Delta m_{kj}^2 L/2E$'s are very small, oscillations are not observable because the probability reduces to $P_{\nu_\alpha \rightarrow \nu_\beta} \simeq \delta_{\alpha\beta}$. Since the LSND experiment has the smallest average L/E , of the order of 1 eV^{-2} , at least one Δm_{kj}^2 , denoted by Δm_{LSND}^2 , must be larger than about 10^{-1} eV^2 in order to generate the observed $\bar{\nu}_\mu \rightarrow \bar{\nu}_e$ and $\nu_\mu \rightarrow \nu_e$ LSND transitions, whose measured probability is of the order of 10^{-3} .

Solar neutrino experiments observe large transitions of ν_e 's into other states, with an average probability of about 1/2. These transitions cannot be generated by a $\Delta m_{kj}^2 \gtrsim 10^{-3} \text{ eV}^2$ because they should have been observed by the long-baseline CHOOZ experiment [10]. Hence, at least another Δm_{kj}^2 smaller than about 10^{-3} eV^2 , denoted by Δm_{SUN}^2 , is needed for the oscillations of solar neutrinos.

The necessary existence of at least a third Δm_{kj}^2 for atmospheric neutrino oscillations is less obvious, but can be understood by noticing that a dependence of the transition probability from the energy E and/or from the distance L is observable only if at least one phase $\Delta m_{kj}^2 L/2E$ is of order one. Indeed, all the exponentials with phase $\Delta m_{kj}^2 L/2E \ll 1$ can be approximated to one, whereas all the exponentials with phase $\Delta m_{kj}^2 L/2E \gg 1$ are washed out by the averages over the energy resolution of the detector and the uncertainty in the source-detector distance. Since the Super-Kamiokande atmospheric

neutrino experiment measures a variation of the oscillation probability for $L/E \sim 10^2 \div 10^3 \text{ eV}^{-2}$ (see Ref.[2]), there must be at least one Δm_{kj}^2 in the range $10^{-3} \div 10^{-2} \text{ eV}^2$, which is out of the ranges allowed for Δm_{SUN}^2 and Δm_{LSND}^2 . Therefore, at least a third Δm_{kj}^2 , denoted by Δm_{ATM}^2 , is needed for atmospheric neutrino oscillations. This argument is supported by a detailed calculation presented in Ref.[11].

In the following sections we discuss some phenomenological aspects of the four-neutrino schemes in Fig.1, in which there are three mass squared differences with the hierarchy (4) indicated by the data.

3. 3+1 Schemes

In 3+1 schemes the amplitude of $\nu_\alpha \rightarrow \nu_\beta$ and $\nu_\beta \rightarrow \nu_\alpha$ transitions in short-baseline neutrino oscillation experiments (equivalent to the usual $\sin^2 2\vartheta$ in the two-generation case) is given by (see, for example, Ref.[4])

$$A_{\alpha\beta} = A_{\beta\alpha} = 4|U_{\alpha 4}|^2|U_{\beta 4}|^2, \quad (6)$$

and the oscillation amplitude (again equivalent to the usual two-generation $\sin^2 2\vartheta$) in short-baseline ν_α disappearance experiments is given

by

$$B_\alpha = \sum_{\beta \neq \alpha} A_{\alpha\beta} = 4|U_{\alpha 4}|^2 (1 - |U_{\alpha 4}|^2). \quad (7)$$

Short-baseline $\bar{\nu}_e$ and ν_μ disappearance experiments put rather stringent limits $B_e \leq B_e^{\text{max}}$ and $B_\mu \leq B_\mu^{\text{max}}$ for $|\Delta m_{41}^2|$ in the LSND-allowed region. Taking into account also the results of solar and atmospheric neutrino experiments, Eq.(7) implies that $|U_{e4}|^2$ and $|U_{\mu 4}|^2$ are small (see Ref.[8] and references therein):

$$|U_{e4}|^2 \leq |U_{e4}|_{\text{max}}^2 \quad \text{and} \quad |U_{\mu 4}|^2 \leq |U_{\mu 4}|_{\text{max}}^2, \quad (8)$$

as shown by the dashed and dotted lines in Figs.2 and 3. These limits imply that the amplitude $A_{\mu e}$, equivalent to the usual $\sin^2 2\vartheta$ in short-baseline $\nu_\mu \rightarrow \nu_e$ and $\bar{\nu}_\mu \rightarrow \bar{\nu}_e$ experiments, is very small:

$$A_{\mu e} \leq 4|U_{\mu 4}|_{\text{max}}^2|U_{e4}|_{\text{max}}^2, \quad (9)$$

so small to be at the border of compatibility with the oscillations observed in the LSND experiment. Figure 4 shows the comparison of the bound (9) with the LSND allowed region, taking into account also the exclusion curves exclusion curves of the KARMEN [14] and BNL-E776 [15]

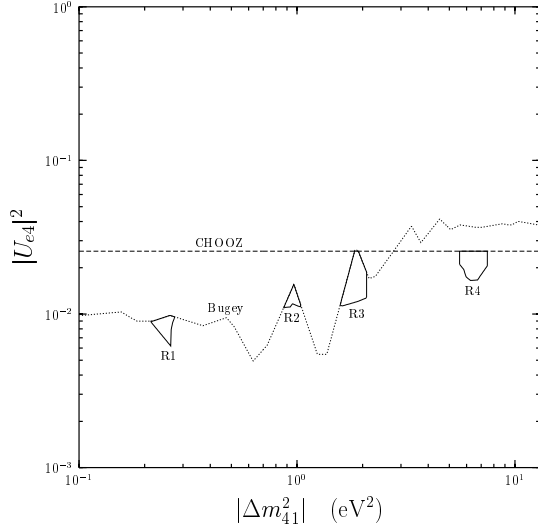


Figure 2. 3+1 schemes. Dotted and dashed lines: $|U_{e4}|_{\text{max}}^2$ from Bugey [12] and CHOOZ [10]. Solid lines enclose the allowed regions.

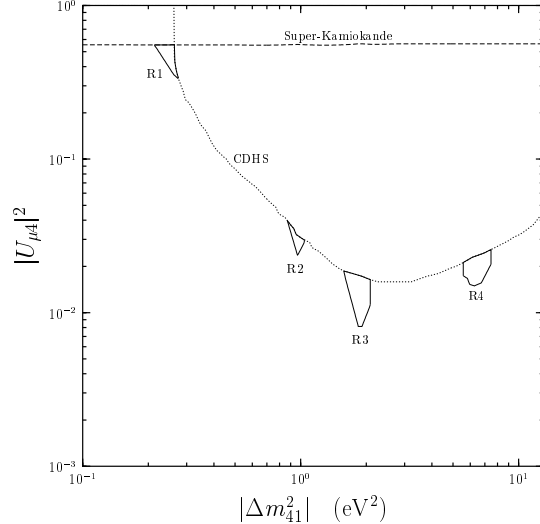


Figure 3. 3+1 schemes. Dotted and dashed lines: $|U_{\mu 4}|_{\text{max}}^2$ from CDHS [13] and Super-Kamiokande [2,6]. Solid lines: allowed regions.

experiments. One can see that there are four regions that are marginally allowed, denoted by R1, R2, R3, R4.

Let us denote by $A_{\mu e}^{\min}$ the lower limit for $A_{\mu e}$ in the four allowed regions in Fig.4. Then, from $A_{\mu e} = 4|U_{\mu 4}|^2|U_{e 4}|^2$ and the upper bounds (8), one can derive lower limits for $|U_{e 4}|^2$ and $|U_{\mu 4}|^2$:

$$|U_{e 4}|^2 \geq \frac{A_{\mu e}^{\min}}{4|U_{\mu 4}|_{\max}^2}, \quad |U_{\mu 4}|^2 \geq \frac{A_{\mu e}^{\min}}{4|U_{e 4}|_{\max}^2}. \quad (10)$$

The upper and lower limits (8) and (10) for $|U_{e 4}|^2$ and $|U_{\mu 4}|^2$ determine the allowed regions enclosed by solid lines in Figs.2 and 3.

Summarizing the general properties of 3+1 schemes obtained so far, from Fig.2 we know that $|U_{e 4}|^2$ is very small, of the order of 10^{-2} , and from Fig.3 we know that in the regions R2, R3, R4 $|U_{\mu 4}|^2$ is also very small, of the order of 10^{-2} , whereas in the region R1 $|U_{\mu 4}|^2$ is relatively large, $0.33 \lesssim |U_{\mu 4}|^2 \lesssim 0.55$. On the other hand, the

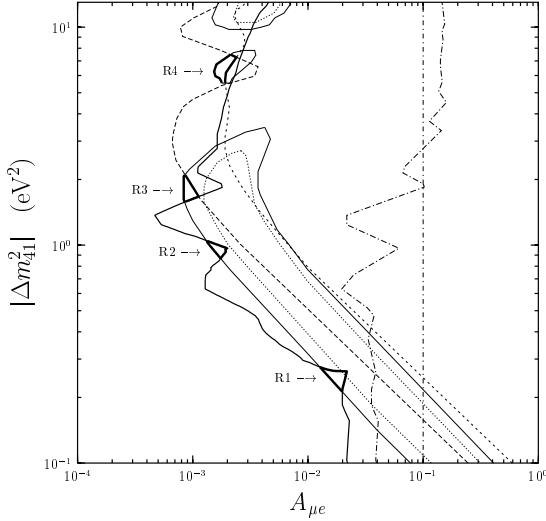


Figure 4. 3+1 schemes. Very thick solid line: allowed regions. Thick solid line: disappearance bound (9). Dotted line: LSND 2000 allowed regions at 90% CL [3]. Solid line: LSND 2000 allowed regions at 99% CL [3]. Broken dash-dotted line: Bugey exclusion curve at 90% CL [12]. Vertical dash-dotted line: CHOOZ exclusion curve at 90% CL [10]. Long-dashed line: KARMEN 2000 exclusion curve at 90% CL [14]. Short-dashed line: BNL-E776 exclusion curve at 90% CL [15].

mixings of ν_τ and ν_s with ν_4 are unknown.

The authors of Ref.[7] considered the interesting possibility that

$$1 - |U_{s 4}|^2 \ll 1, \quad (11)$$

i.e. that the isolated neutrino ν_4 practically coincides with ν_s . Notice, however, that $|U_{s 4}|^2$ cannot be exactly equal to one, because LSND oscillations require that $|U_{e 4}|^2$ and $|U_{\mu 4}|^2$ do not vanish, as shown in Figs.2 and 3, and unitarity implies that $1 - |U_{s 4}|^2 \geq |U_{e 4}|^2 + |U_{\mu 4}|^2$. The possibility (11) is attractive because it represents a perturbation of the standard three-neutrino mixing in which a mass eigenstate is added, that mixes mainly with the new sterile neutrino ν_s and very weakly with the standard active neutrinos ν_e, ν_μ, ν_τ . In this case, the usual phenomenology of three-neutrino mixing in solar and atmospheric neutrino oscillation experiments is practically unchanged: the atmospheric neutrino anomaly would be explained by dominant $\nu_\mu \rightarrow \nu_\tau$ transitions, with possible sub-dominant $\nu_\mu \leftrightarrow \nu_e$ transitions constrained by the CHOOZ bound, and the solar neutrino problem would be

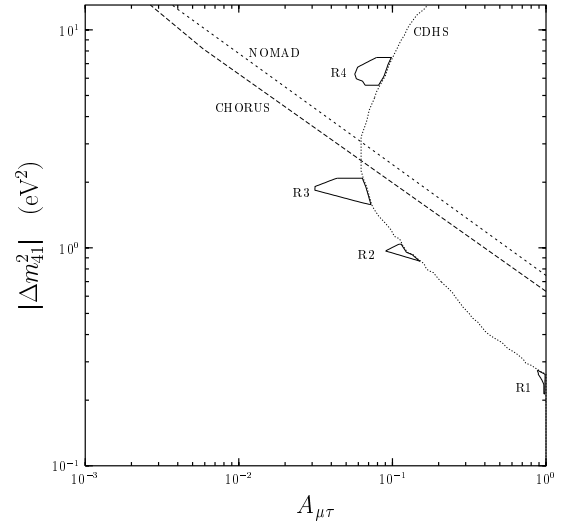


Figure 5. 3+1 schemes with $|U_{s 4}|^2 \ll 1$. Solid lines enclose the allowed regions. Long dashed line: CHORUS exclusion curve at 90% CL [16]. Short dashed line: NOMAD exclusion curve at 90% CL [17]. Dotted line: CDHS exclusion curve at 90% CL [13].

explained by an approximately equal mixture of $\nu_e \rightarrow \nu_\mu$ and $\nu_e \rightarrow \nu_\tau$ transitions (see, for example, Ref.[4]). An appealing characteristic of this scenario is the practical absence of transitions of solar and atmospheric neutrinos into sterile neutrinos, that seems to be favored by the latest data (see [18,2,19]).

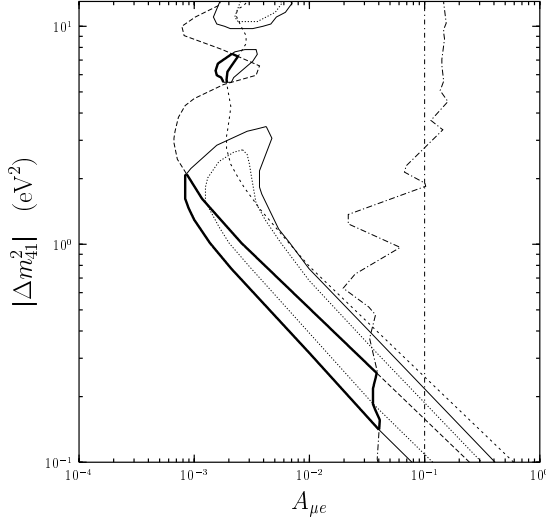


Figure 6. 2+2 schemes. See caption of Fig.4.

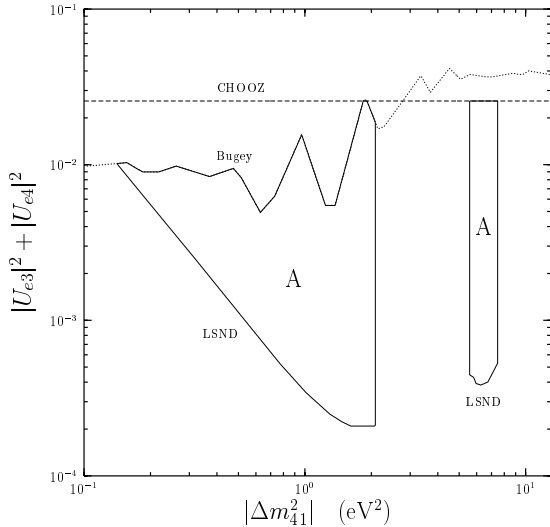


Figure 7. 2+2 schemes. Dotted and dashed lines: upper limit from Bugey [12] and CHOOZ [10]. The regions marked by “A” enclosed by solid lines are allowed.

Another interesting possibility has been considered in Ref.[8]:

$$|U_{s4}|^2 \ll 1. \quad (12)$$

This could be obtained, for example, in the hierarchical scheme I (see Fig. 1) with an appropriate symmetry keeping the sterile neutrino very light, *i.e.* mostly mixed with the lightest mass eigenstates. Notice that nothing forbids $|U_{s4}|^2$ to be even zero exactly. The possibility (12) is interesting because if it is realized there are relatively large $\nu_\mu \rightarrow \nu_\tau$ and $\nu_e \rightarrow \nu_\tau$ transitions in short-baseline neutrino oscillation experiments, that could be observed in the near future. This is due to the fact that the unitarity of the mixing matrix implies that $|U_{\tau 4}|^2$ is large ($1 - |U_{\tau 4}|^2 \ll 1$ in the regions R2, R3, R4 and $0.45 \lesssim |U_{\tau 4}|^2 \lesssim 0.67$ in the region R1). Therefore, the amplitudes $A_{\mu\tau} = 4|U_{\mu 4}|^2|U_{\tau 4}|^2$ and $A_{e\tau} = 4|U_{e 4}|^2|U_{\tau 4}|^2$ of short-baseline $\nu_\mu \rightarrow \nu_\tau$ and $\nu_e \rightarrow \nu_\tau$ oscillations are suppressed only by the smallness of $|U_{\mu 4}|^2$ and $|U_{e 4}|^2$ and lie just below the upper limits imposed by the negative results of short-baseline ν_μ and $\bar{\nu}_e$ disappearance experiments. Figure 5 shows the allowed regions in the $A_{\mu\tau}$ - $|\Delta m_{41}^2|$ plane. One can see that the region R4 is excluded by the neg-

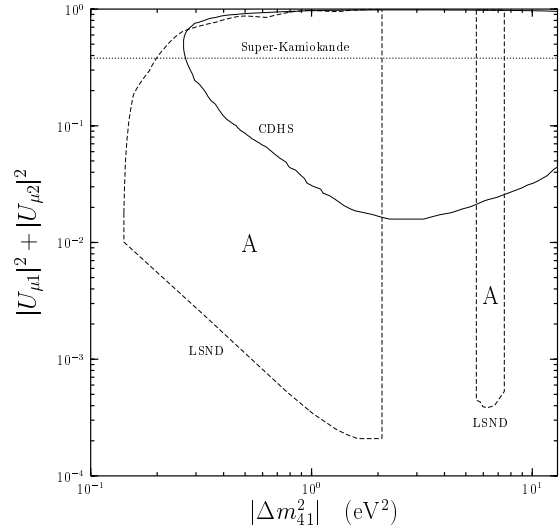


Figure 8. 2+2 schemes. Solid, dotted and dashed lines: limits from CDHS [13], Super-Kamiokande [2,6] and LSND [3,20]. The allowed regions are marked by “A”.

ative results of the CHORUS [16] and NOMAD [17] experiments. The other three regions are possible and predict relatively large oscillation amplitudes that could be observed in the near future, especially the two regions R2 and R3 in which $A_{\mu\tau} \sim 4 \times 10^{-2} - 10^{-1}$. An unattractive feature of this scenario is its predictions of large $\nu_\mu \rightarrow \nu_s$ transitions of atmospheric neutrinos, that appear to be disfavored by the latest data (see [2,19]).

4. 2+2 Schemes

The two 2+2 schemes in Fig. 1 are favored by the data because they do not suffer the constraint imposed by the thick solid line in Fig.4, that is valid only in 3+1 schemes. Therefore, all the part of the LSND region in the $A_{\mu e}-\Delta m_{41}^2$ plane that is not excluded by other experiments is allowed, as shown in Fig.6. For this reason, the phenomenology of 2+2 schemes has been studied in many articles [5].

Figures 7 and 8 show the limits on the mixing of ν_e and ν_μ obtained from the results of short-baseline, solar and atmospheric experiments [5, 20]. From Fig. 7 one can see that the mixing of ν_e with ν_3 and ν_4 , whose mass-squared difference Δm_{43}^2 generates atmospheric neutrino transitions, is very small, leading to a suppression of oscillations of ν_e 's in atmospheric and long-baseline experiments [21].

The mixing of ν_τ and ν_s is almost unknown, with weak limits obtained in recent fits of solar [22] and atmospheric data [23,24]. For example, it is possible that both solar ν_e 's and atmospheric ν_μ 's oscillate into approximately equal mixtures of ν_τ and ν_s 's.

In the future it may be possible to exclude the scheme A if it will be established with confidence that the effective number of neutrinos in Big-Bang Nucleosynthesis is less than four. In this case $|U_{s3}|^2 + |U_{s4}|^2 \ll 1$ [25] and solar and atmospheric neutrino oscillations occur, respectively, through the decoupled channels $\nu_e \rightarrow \nu_s$ and $\nu_\mu \rightarrow \nu_\tau$. It has been shown that in this scenario the small mass splitting in scheme A between ν_3 and ν_4 is incompatible with radiative corrections [26] and the effective Majorana mass in neutrinoless double-beta decay in scheme A is

at the border of compatibility with the experimental limit [27].

5. Conclusions

Four-neutrino mixing is a realistic possibility (if the solar, atmospheric and LSND anomalies are due to neutrino oscillations). It is rather complicated, but very interesting, both for theory and experiments, because: it has a rich phenomenology; the existence of a sterile neutrino is far beyond the Standard Model, hinting for exciting new physics; there are several observable oscillation channels in short-baseline and long-baseline experiments; CP violation may be observable in long-baseline experiments [5].

REFERENCES

1. A.Yu. Smirnov, these proceedings.
2. T. Kajita, these proceedings.
3. P. Spentzouris, these proceedings.
4. S. M. Bilenky, C. Giunti, and W. Grimus, Prog. Part. Nucl. Phys. **43**, 1 (1999).
5. Reference list at www.to.infn.it/~giunti/4nu.
6. S. M. Bilenky, C. Giunti, W. Grimus, and T. Schwetz, Phys. Rev. **D60**, 073007 (1999).
7. V. Barger *et al.*, Phys. Lett. **B489**, 345 (2000).
8. C. Giunti and M. Laveder, hep-ph/0010009.
9. O. Peres and A. Smirnov, hep-ph/0011054.
10. M. Apollonio *et al.*, Phys. Lett. **B466**, 415 (1999).
11. G. L. Fogli *et al.*, hep-ph/9906450.
12. Y. Declais *et al.*, Nucl. Phys. **B434**, 503 (1995).
13. F. Dydak *et al.*, Phys. Lett. **B134**, 281 (1984).
14. M. Steidl, these proceedings.
15. L. Borodovsky *et al.*, Phys. Rev. Lett. **68**, 274 (1992).
16. P. Zucchelli, these proceedings.
17. G. Vidal-Sitjes, these proceedings.
18. Y. Suzuki, these proceedings.
19. F. Ronga, these proceedings.
20. C. Giunti, JHEP **0001**, 032 (2000).
21. S.M. Bilenky, C. Giunti and W. Grimus, Phys. Rev. **D57**, 1920 (1998).
22. M.C. Gonzalez-Garcia and C. Pena-Garay, hep-ph/0011245.
23. O. Yasuda, hep-ph/0006319.

- 24. G.L. Fogli *et al.*, hep-ph/0009299.
- 25. N. Okada and O. Yasuda, Int. J. Mod. Phys. A **12**, 3669 (1997).
- 26. A. Ibarra and I. Navarro, JHEP **0002**, 031 (2000).
- 27. C. Giunti, Phys. Rev. **D61**, 036002 (2000).